Geologica Acta, Vol.9, Nº 1, March 2011, 67-77
DOI: 10.1344/105.000001652
Available online at www.geologica-acta.com

geologica acta

Calcite dissolution by mixing waters: geochemical modeling and flow-through experiments

E. SANZ |1| **C. AYORA** |2| **J. CARRERA** |1|

|1| **ExxonMobil Upstream Research Company**
Houston, Texas, USA E-mail: esteban.sanz@live.com

|2| **Institute of Enviromental Assessment and Water Research, IDAEA-ECSIC**
Barcelona, Spain

ABSTRACT

Dissolution of carbonates has been commonly predicted by geochemical models to occur at the seawater-freshwater mixing zone of coastal aquifers along a geological time scale. However, field evidences are inconclusive: dissolution vs. lack of dissolution. In this study we investigate the process of calcite dissolution by mixing waters of different salinities and p_{CO2}, by means of geochemical modeling and laboratory experiments. Our calculations show that saturation is not always a good indicator of the real dissolution potential of the mixture. In a closed system, the maximum subsaturation occurs for mixing ratios of about 15%-salty, while the dissolved calcite is maximum for 50%. Dissolution is affected by carbonate speciation, and by the dependence of activity coefficients on salinity. Laboratory experiments confirmed a strong dependence of the dissolution on the mixing ratio and pointed out the critical role of CO_2 variations at the local atmosphere. The maximum dissolution was observed for mixtures less than 17%-salty, which is attributed to the CO_2 exchange between the reaction cell and the laboratory atmosphere. The reaction cell gains CO_2 for mixtures less than 17%-salty and calcite dissolution is enhanced with respect to a closed system. The opposite also occurs for mixtures higher than 17% salty. Including CO_2 exchange, the model consistently predicts the experimental results. Both calculations and dissolution experiments at different flow rates demonstrated a high sensitivity of the amount of calcite dissolved to minor variations of CO_2 partial pressure of the local atmosphere. This could be relevant in field scale interpretations. CO_2 pressure measurements in the field are not easy to obtain and could account for the different and "contradictory" field observations.

KEYWORDS | **Calcite dissolution. Mixing waters. Flow-through experiments. Seawater intrusion. Geochemical modeling.**

INTRODUCTION

Mixing of calcite-saturated groundwaters may result in undersaturated solutions with a potential for calcite dissolution in carbonate formations. This undersaturation is caused by the combination of a number of factors. Of those factors, algebraic, salinity, p_{CO2}, pH and temperature are the most relevant (Wigley and Plummer, 1976). The algebraic effect is due to the non-linearity of product of species concentrations in a mixture compared to the linear variation of total concentrations. If the product of reactants concentrations is the same for two mixing waters, such

product will be larger for any mixture. If ion activity coefficients are assumed constant, the ion activity product (IAP) of any mixture is always higher than the equilibrium constant. This causes oversaturation of mixtures, even if the end members are in equilibrium (Fig. 1A).

The salinity effect (also called Ionic strength effect) occurs when two solutions with different salinity are mixed together. The resulting solution is subsaturated in calcite as a result of the non-linear dependence of the ion activity coefficients on ion strength especially at low to moderate ion strengths. Because the activity coefficient of ions in a mixture is lower than the linear combination of the activity coefficients of end-member solutions, the mixture presents a higher solubility of calcite and is therefore undersaturated (Fig. 1B).

The saturation of a mixture also depends on the pH and p_{CO2} because of the strong dependence of the carbonate species on pH (Fig. 1C). Thus, the CO_3^{2-} concentration will be higher under slightly basic conditions than under acidic ones. Therefore, the mixture of slightly acidic fluids will be more easily subsaturated than the mixture of more basic ones. Finally, temperature variations may also affect the saturation of a mixture because of the non-linear dependence of the mineral equilibrium constants on temperature. However, in non-geothermal groundwaters, temperature variations exceeding 10ºC are not expected within the range of a few meters (the scale of the carbonate cavities) and the temperature effect becomes practically negligible in such environments (Corbella and Ayora, 2003).

The theory of carbonate subsaturation by mixing has been extensively used to interpret carbonate dissolution textures in caves and borehole samples from coastal environments (Plummer, 1975). Additionally, reactive transport modeling exercises have shown that significant porosity development may occur at the salt water-fresh water mixing zone of coastal aquifers along a geological time scale (Sanford and Konikow, 1989; Rezaei et al., 2005, Romanov and Dreybrodt, 2006). Mixing of two fluids with different salinity has also been used to account for deep dissolution of carbonates and the formation of hydrothermal mineral deposits (Corbella et al., 2004, 2006).

Field evidence is, however, inconclusive. Observation of mixing and carbonate dissolution at depth has not been possible because of technical difficulties. More accessible to observation is the seawater mixing zone in coastal aquifers where calcite undersaturation and/or calcite dissolution have been reported numerous times (Back et al., 1979; Hanshaw and Back, 1980; Back et al., 1986; Smart et al., 1988; Stoessell et al., 1989; Ng and Jones, 1995; Whitaker and Smart, 1997). However, dissolution in coastal environments is not always clear cut. The absence of undersaturation (Plummer et al., 1976; Magaritz and Luzier, 1985; Price and Herman, 1991; Wicks et al., 1995; Pulido-Leboeuf, 2004) or a lack of correlation between changes in cement type or porosity development and current locations of mixing zones have also been described (Maliva et al., 2001; Melim et al., 2002). Moreover, evidence of dissolution admits alternative explanations. For example, sea level oscillated tens of meters during the Pleistocene, causing diluted continental water to invade and dissolve carbonate aquifers in the areas where prior or subsequent salt water intrusion and mixing occurred. Therefore, dissolution features in carbonates do not necessarily mean that dissolution occurs under mixing conditions. In summary, laboratory experiments are needed to validate the reliability of model predictions.

The only reported laboratory experiments of carbonate reaction by mixing saturated solutions have been performed by Singurindy et al. (2004). These authors used a 2D flow cell filled with crushed calcite in which two solutions were injected at different flow rates along

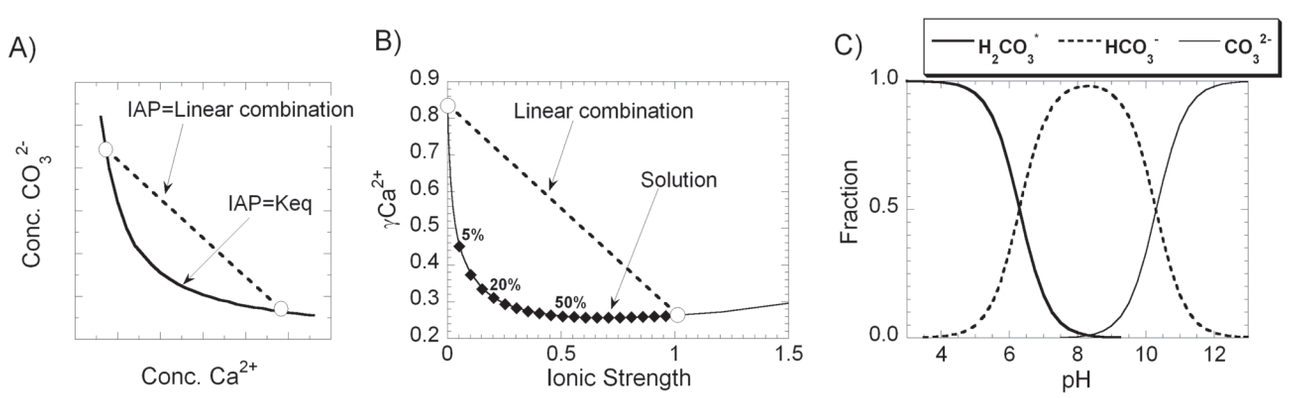

FIGURE 1 | **Schemes illustrating three of the most relevant factors affecting calcite saturation of a mixture of two calcite-saturated solutions. A) the algebraic effect. B) the salinity effect (the labels % indicate the proportion of of a 1m NaCl-solution in the mixture). C) pH and pCO_2 effect.**

two cell faces, while the other two faces allowed mixed solution outflow. End-member solutions were deionized water and 40g/L NaCl solution both equilibrated with calcite at room temperature and atmospheric CO_2 partial pressure. For input mixing ratios of 30 and 50% of saline water dissolution occurred as evidenced by an increase in the measured Ca concentration in the outlet solution. They observed higher dissolution for the 30%-salty mixing and results were in agreement with predictions made with a simple transport model. However, because of the limitations of the experiment design, no quantitative relationship of subsaturation and dissolution extent was shown. Indeed, mixing subsaturation and dissolution did not occur uniformly throughout the flow cell.

It may be concluded that neither field observations nor laboratory experiments have allowed a detailed comparison between subsaturation predictions and observations of current calcite dissolution. Thus, the objective of the present work is twofold:

- To test numerically the relationship of calcite saturation and potential dissolution with the mixing proportion of two end-member solutions equilibrated with calcite.

- To compare the predictions of calcite dissolution with laboratory results from flow-through experiments with variable p_{CO2} and a range of mixing ratios.

MODELING OF CALCITE SATURATION AND DISSOLUTION

It is generally assumed that the degree of subsaturation of a solution is a direct estimator of its potential for mineral dissolution. However, the discussion below demonstrates that this is not necessarily so. We developed a simple calculation consisting of mixing two calcite-saturated end-member solutions at different mixing proportions in a closed system, and allowed the mixture to dissolve calcite up to equilibrium. These simulations were performed with PHREEQC and the Pitzer ion-ion interaction coefficients (Parkhurst and Appelo, 2006). The selection of the two end-member solutions (Table 1) was inspired on a plausible seawater intrusion mixing zone in natural coastal aquifers (Rezaei et al., 2005). However, the seawater was replaced by a solution with higher ionic strength in order to enhance the salinity effect and subsaturation in this study. The composition of the salty solution was pure NaCl to reduce ion-pair effects and complexity of interpretation.

Simulation results are presented in Fig. 2 in terms of calcite saturation and mass of dissolved calcite with respect to the mixing ratio. The maximum dissolution is calculated to occur for a mixing ratio of about 50% while the highest subsaturation is obtained for a mixing ratio of 15-20%.

In order to gain some insight into this paradox, we first defined the overall dissolution reaction considered for calcite, as

$$CaCO_3 \rightarrow Ca^{2+} + CO_3^{2-} \quad (1)$$

Then, we computed the activities of the species controlling dissolution, Ca^{2+} and CO_3^{2-}, for both input mixtures and equilibrium solutions, in steps of 5% mixing ratio. Results are given in Fig. 3A. The different input mixtures display very similar CO_3^{2-} activity and a wide range of Ca^{2+} activities. Note that carbonate activities are about two orders of magnitude smaller than those of calcium, because the dominant species at the mixing pH is bicarbonate (Fig. 1C). Calcite subsaturation increases towards the fresh end-member, where activity coefficients drop sharply as salinity increases (Fig. 1B).

Concentrations (and thus activities) of calcium and carbonate in solution increase when calcite dissolves congruently. The moderate value of pH (note that the pH of

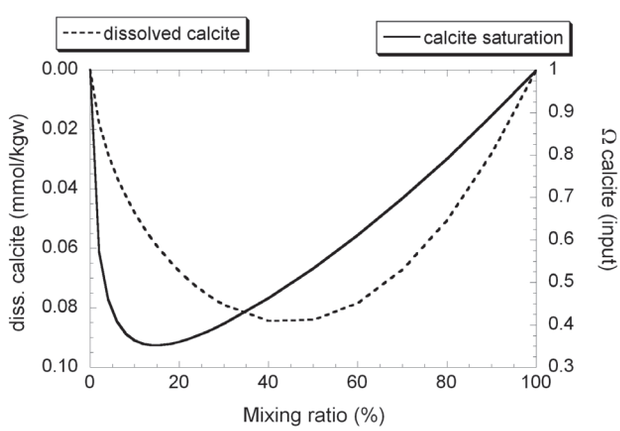

FIGURE 2 | **Computed input saturation state and dissolved calcite after reaction to equilibrium for mixtures of the two solutions described in Table 1. Salinity increases on the right.**

TABLE 1 | **Input end-member solutions used in the experiments and numerical simulations. Ω accounts for saturation, and I for ionic strength.**

Name	pH	Ca tot (m)	Na tot (m)	Cl tot (m)	-log(p_{CO2})	Ω calcite	I
Fresh solution	8.3	5.29×10^{-4}	0.0	0.0	3.5	1.0	0.002
Salty solution	7.38	3.70×10^{-3}	1.0	1.0	2.0	1.0	1.01

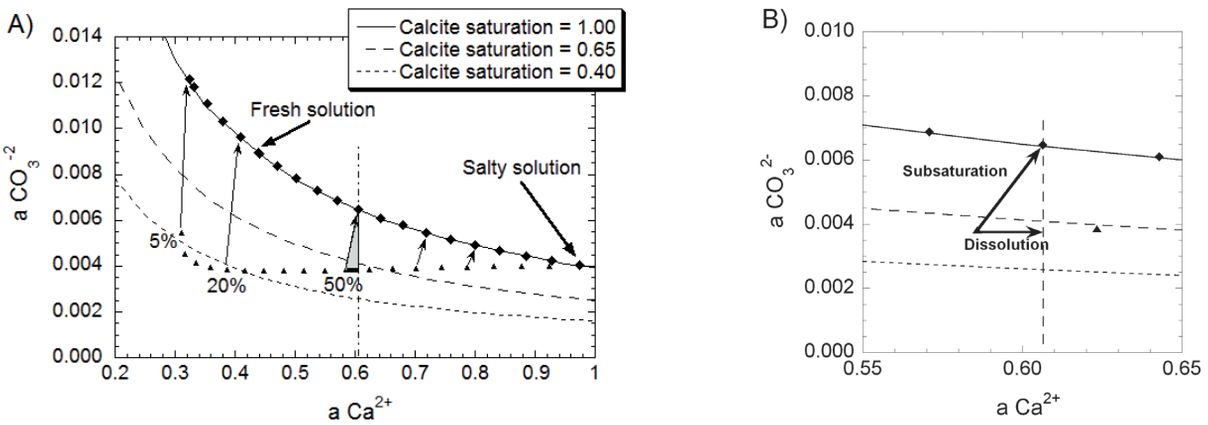

FIGURE 3 | **A) Relationship of calculated activities of Ca^{2+} and CO_3^{2-} in the mixed solutions. Solutions are calculated every 5% of mixing ratio. Triangles depict the mixed input solutions and filled diamonds the mixed solutions after reaction to equilibrium. Arrows indicate the evolution of the composition with dissolving calcite. The curves represent several calcite saturation values. Note the dramatic reduction in the activities of Ca^{2+} and CO_3^{2-} after the first salinization step. B) Enlargement of the previous figure shows the extent of subsaturation and dissolution.**

end members is 8.30 and 7.38; see Table 1) causes most dissolved carbonate to become bicarbonate (this is why the activity of CO_3^{2-} is two orders of magnitude lower than that of Ca). As shown in Fig. 3A, dissolution of calcite increases from 0 to 20%-salty mixtures because of the decrease in saturation. This reduction reflects the large reduction in activity coefficients caused by the increase of salinity and the reduction of carbonate concentration caused by speciation. For mixtures richer in saline water, subsaturation begins to decrease as salinity increases. However, total dissolution continues to increase, as evidenced by the higher value of the Ca-component of the vector leading to saturation in Fig. 3B. This component measures the amount of Ca^{2+} activity required to reach equilibrium. The amount of calcite dissolution is in fact measured by the increment in Ca concentration of the solution, and can be considered roughly proportional to the Ca^{2+} activity variation. Note that the activity coefficients of ions decrease with salinity and that the differences between concentration of calcium in solution and its activity are also larger. However, for mixtures with more than 50% of saline water this effect is negligible (Fig. 1B), the saturation state approaches to unity and less calcite is dissolved.

EXPERIMENTS: MATERIALS AND METHODS

Experimental setting

Dissolution experiments were carried out using 35mL flow-through Lexan reactor cells (Metz and Ganor, 2001) at a temperature of 25 ±1.5 ºC. Flow-through experiments allowed us to measure dissolution rate under different flow rates (i.e., residence time) and initial powder mass (i.e., water/rock ratio). Inside the cell, calcite reacted with a through-flowing fixed mixture of two end-member solutions with different salinities. Each of these end-member solutions was equilibrated with calcite and a certain p_{CO2} in separate hermetic reservoirs prior to mixing (Fig. 4). Equilibrium with calcite was ensured by adding calcite powder (Merck, pro analysis quality, 99.0% purity, impurities not relevant) in excess to the reservoirs, and by maintaining the solutions constantly stirred with a magnet inside the reservoir tanks with a residence time of 1 to 2 days. Commercial N_2-CO_2 gas mixtures were bubbled into the reservoirs for two hours twice a day. This was sufficient to maintain calcite-equilibrium at the desired CO_2 pressure, as proved in preliminary tests by measuring pH and Ca and Na concentration (see Table 1).

Tank solutions were pumped into a mixing cell. Before entering the mixing cell, solutions were filtered through a 0.45μm filter to prevent suspended calcite particles from entering the tubing system (Fig. 4). A set of preliminary

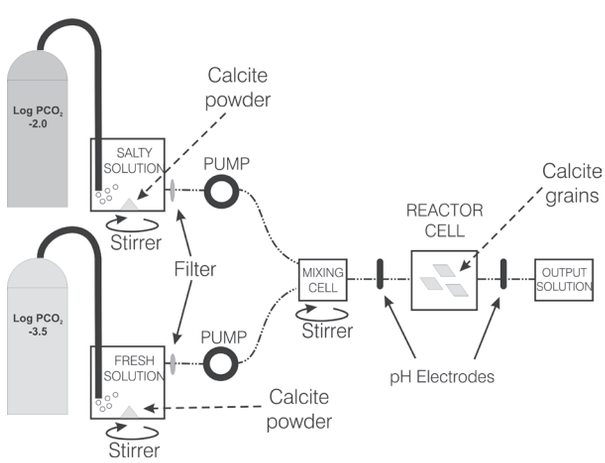

FIGURE 4 | **General experimental set-up showing the flow-through system used in the present study.**

tests (not shown) were performed to confirm that solution reservoirs, connections and tubes (made of PVC) were practically impervious to CO_2 diffusion. However, as discussed below, the reactor cells allowed some gas transfer with the laboratory atmosphere. The CO_2 in the laboratory presented a stable pressure of $10^{-3.22}$ ±10% bar over the duration of the experiments. Note that this is higher than standard atmospheric pressure. The p_{CO2} measurement was obtained from the barometric pressure and an infra-red analyzer Anagas CD 98 plus.

Stable flow rate and fixed mixing ratios were achieved combining two peristaltic pumps running at different rates and/or using pumping tubes of different diameters. Flow rate was double checked by volume-weighted output solution every 8h. Although flow rates ranged from 0.05 to 0.6mL/min ($8.33x10^{-7}$ to $1.00x10^{-5}$kgw/s), 0.1mL/min ($1.66x10^{-6}$kgw/s) was mostly used in the experiments (see Table 2 for details). pH was continuously measured in-situ upstream and downstream of the reactor cell using sealed cells with a glass combined electrode (Orion #9157BN Triode™) interfaced with a computer (through a Orion 720A pH meter). These measurements correspond to mixed-input and reaction pH, respectively (Fig. 4). The calibration of pH electrodes was verified against standard buffer solutions of pH 7.00 and 9.21 every 24h.

Experiments consisted of one or several sequential stages. When sequential stages were considered, solid was not changed but the flow rate or mixing ratios varied (Table 2). Experiments were run for every stage until steady flow rate, mixing ratio and input and output Ca concentrations were observed for a minimum of 32h (four consecutive samples). Thereafter, they were stopped or the conditions were modified to a new stage. The design of the experiment ensured that steady state was rapidly achieved and that the stages lasted no longer than 9 days. Each experiment was subject to a pre-reaction period (with the reactor cell not connected to the system) to allow the system to reach stable flow rate and a mixing ratio before reaction occurred. In one experiment (Exp-03_p1, Table 2), the flow was stopped and the reactor cell was sealed for 60 h and behaved as a batch experiment. The concentration in the cell was measured at the end of this period.

TABLE 2 | **Experimental conditions and results of the flow-through experiments. Values of flow rate, mixing ratio, Ca inp, Ca out and ΔCa are measured at steady-state conditions of the experiment.**

Experiment	Duration (h)	Grain size (μm)	Initial mass (g)	Flow rate (mL/min)	Mixing ratio (%)	Ca inp (mmol/kgw)	Ca out (mmol/kgw)	Δ Ca (mmol/kgw)
Exp-01	111	125-250	0.5029	0.61	16.7	0.878	0.893	0.015
Exp-02_b	36	125-250	0.5039	0.10	14.4	0.952	0.974	0.022
Exp-02_c	44	125-250		0.31	14.5	0.929	0.940	0.011
Exp-03_a	142	25-53	0.6053	0.09	14.4	0.942	1,100	0.158
Exp-03_b	60	25-53		0.11	12.9	0.909	1,022	0.113
Exp-03_p1	60	25-53		0.00	12.9	0.909	1,089	0.180
Exp-03_d	50	25-53		0.10	13.4	0.936	1,036	0.101
Exp-04_a	216	25-53	0.6083	0.10	13.4	0.919	1,011	0.092
Exp-05_a	66	25-53	0.6020	0.10	49.4	1,824	1,842	0.018
Exp-05_b	48	25-53		0.09	47.3	1,801	1,841	0.040
Exp-06	165	25-53	0.6027	0.09	20.7	1,108	1,167	0.060
Exp-07_b	107	25-53	0.6003	0.09	21.2	1,153	1,196	0.043
Exp-07_c	97	25-53		0.10	40.7	1,680	1,708	0.027
Exp-08_a	144	25-53	0.6019	0.09	5.2	0.718	0.747	0.028
Exp-08_b	114	25-53		0.09	7.4	0.777	0.837	0.060
Exp-08_c	114	25-53		0.05	7.4	0.771	0.889	0.117

Solid and solution characterization

The calcite sample used in this study is Iceland spar from a skarn deposit in Martinet (Eastern Pyrenees, Spain) containing only $CaCO_3$ (based on X-ray diffraction analysis). A polished section of the calcite crystal was analyzed with Electron Microprobe (Wavelength Dispersive Analysis). The concentration of cations other than Ca was all below the detection limit (0.05 wt %). The crystal was ground with an agate mortar and sieved to fractions 125-250μm and 25-53μm. The BET initial surface area for these size fractions was 0.17 and 0.21m^2/g, respectively (measured using 5-point N_2 adsorption isotherms). We assumed that the surface area did not change significantly during the experiments because of the small amount of calcite dissolved. Scanning Electron Microscope (SEM) photographs of the initial raw material showed that the rhombohedral shape of the calcite crystals, as well as clean surfaces and sharp edges, were mostly preserved after grinding (Fig. 5A). Most of the experiments were designed with the same grain size (25-53μm) and initial mass of calcite (approximately 0.6g) to facilitate comparison of results (Table 2). When an experiment was stopped, the reactor was immediately dismantled and the remaining calcite powder was recovered, cleaned with ethanol and stored in a dry atmosphere. The recovered powder was then weighted and examined by SEM in order to quantify the effect of dissolution on crystal surfaces. Recovered mass of calcite represented 90 to 95% of the initial mass in all cases.

All the experiments were run using the same end-member solutions, but mixed in different proportions. Fresh input solution consisted of double deionized water equilibrated with calcite and with a p_{CO2} of $10^{-3.5}$bar (i.e. the standard CO_2 content in the atmosphere). The salty input solution was prepared equilibrating a 1m NaCl solution (from Merck, pro analysis quality, 99.5% purity, impurities not relevant) with calcite and a p_{CO2} of $10^{-2.0}$bar (Table 1). A volume of 5mL of input end-member solutions were sampled and analyzed every 24h over the duration of the experiments to check the stability of the input solution and detect any possible variation in the experimental conditions. Also 5mL of the output solution was sampled every 8h in all the experiments. All input and output samples were analyzed for pH, and Ca and Na concentrations. Ca and Na concentrations were analyzed with ICP-AES. Analytical error in these techniques was 0.02 for pH and 3% for cations.

Measurement of dissolved calcite

The mixing ratio (salt term fraction), θ, in the ith sample was obtained from sodium concentrations:

$$\theta_i = \frac{C_{Na,i-out} - C_{Na,fresh}}{C_{Na,salty} - C_{Na,fresh}} \quad (2)$$

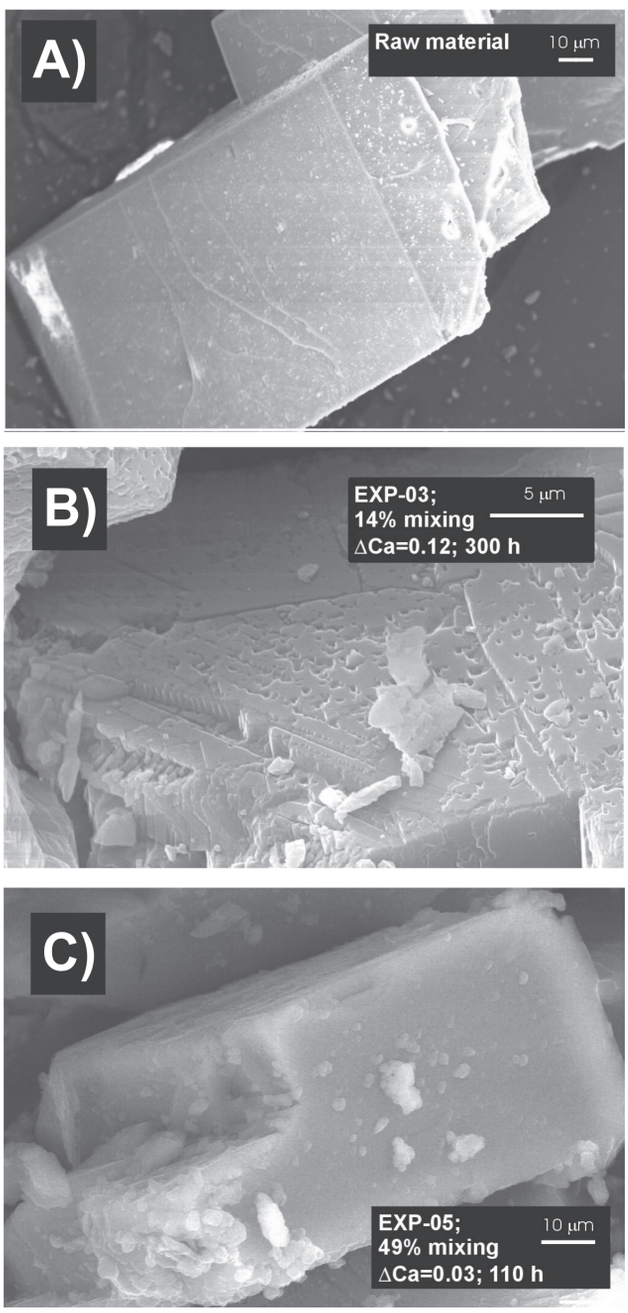

FIGURE 5 | **SEM microphotographs: A) Raw calcite grains. B) Recovered material from Exp-03 (14%). Dissolution is characterized by the development of etch pits that can often grow following preferential crystallographic planes (likely exfoliation) by lateral migration or intersect ending in organized linear or curvilinear trench-like chains. C) Recovered material from Exp-05 (49%), crystals show no dissolution, although crystal edges are clearly rounded.**

where $C_{Na,fresh}$, $C_{Na,salty}$ and $C_{Na,i-out}$ represent the sodium concentration in the fresh end-member (mol/kgw), the salty end-member and the ith output solutions, respectively. Ca concentration in the ith mixed-input solution, $C_{Ca,i-inp}$, is obtained from the mixing ratio as:

$$C_{Ca,i-inp} = \theta_i C_{Ca,salty} + (1-\theta_i) C_{Ca,fresh} \quad (3)$$

where $C_{Ca,fresh}$ and $C_{Ca,salty}$ represent the calcium concentration in the fresh and salty end member solutions, respectively. Dissolution of calcite for different mixing ratios was determined from the observation of dissolution features on the crystal surfaces under SEM, and quantified by the increase of Ca in solution after reaction.

Experimental conditions were designed to reach a compromise between initial mass, calcite grain size, and residence time in the reactor cell, and were tested in a series of preliminary tests. It was not easy to obtain a stable signal of input and output pH in the system. Although the pH after reaction was higher than in the input solution for all cases, the uncertainty associated with the measurement prevented an accurate evaluation of the calcite saturation in the reactor cell. The uncertainties account for instability in the signal, which can be attributed to small variations of flow and temperature on the probe. Further, experimental conditions were modelled with the reactive transport code RETRASO (Saaltink et al., 2004) and the Pitzer ion-ion interaction coefficients (Harvie et al., 1984) to confirm that calcite equilibrium was achieved in all cases. The code simulated kinetic dissolution of calcite following the dissolution rate of Arvidson et al. (2003) of $10^{-10.95}$mol/cm^2/s obtained from dissolution at calcite crystal surfaces. Thus, the output Ca concentration when the system reaches steady state can be calculated from:

$$\frac{\partial c_{Ca,out}}{\partial t} = 0 = \frac{c_{Ca,inp} - c_{Ca,out}}{t_R} - kAf(1-\Omega) \quad (4)$$

where t_R is the residence time in the reactor cell (s), k is the calcite dissolution rate constant (mol/m^2/s), A is the reactive surface area (m^2/g), f is the solid:solution ratio in the reactor cell (g/L) and Ω is the calcite saturation of the solution. Eq. 4 allows the calculation of Ω as a function of the experimental conditions. Fig. 6 displays Ω versus the specific surface for a flow rate of 1.70x10^{-6}kgw/s (0.1mL/min), a 15%-salty mixing ratio and a solid solution ratio of 0.6g : 0.035L reactor cell. As shown in Fig. 6, the time lasted by the experiments is about two orders of magnitude longer than that required to reach equilibrium. Since the modelled case of 15% mixing ratio resulted in the highest subsaturation, we can conclude that all the experiments reached calcite-solution equilibrium.

The experimental results are presented in terms of the increase in Ca concentration during reaction (equivalent

to dissolved calcite, *Diss.cc.*, if congruent dissolution is assumed) as:

$$Diss.cc. = C_{Ca,out} - C_{Ca,inp} \quad (5)$$

and the associated error:

$$\delta_{Diss.cc} = \left(\delta^2_{C_{Ca,out}} + \delta^2_{C_{Ca,inpt}}\right)^{1/2} \quad (6)$$

where $\delta_{Diss.cc}$, $\delta_{C_{Ca,out}}$ and $\delta_{C_{Ca,inpt}}$ represent the errors associated with dissolved calcite and Ca output and input concentrations, respectively.

EXPERIMENTAL RESULTS

Dissolution experiments covered the range of 0-50%-salty mixing ratios and all mixing ratios were tested at least twice. Dissolution was observed in all the experiments, but its extent varied with the mixing ratio. Experimental results are compiled in Table 2. The time evolution of flow rate, mixing ratio and Ca concentration in two representative experiments is depicted in Fig. 7, where negative times indicate pre-reaction conditions. Differences between input and output calcium concentration in some experiments were within analytical error, which reflects the low potential of calcite dissolution associated to mixtures of two waters initially in equilibrium with calcite. Still, such results were used in the discussion because these differences were consistent and stable in time.

SEM microphotographs of the calcite are in agreement with the increase in Ca concentration observed. Dissolution evidences were identified on the surface of all the recovered calcite grains and the observation of dissolution features on crystal surfaces validated qualitatively the existence of calcite dissolution. For experiments with the highest increase in Ca, dissolution was characterized by the development of etch pits that often grew following preferential crystallographic planes (likely exfoliation) (Fig. 5B). When a lower increase in Ca concentration was observed, etch pits were not found and dissolution yielded non-geometrical corrosion features that did not reproduce crystal structures. Finally, in the experiments with the lowest release of Ca, the calcite crystals did not show dissolution patterns in their faces, but the crystal edges were clearly rounded with respect to the initial material (Fig. 5C). These observations are in agreement with the behaviour of calcite dissolution for different subsaturation values observed under Atomic Force Microscopy (Arvidson et al., 2003).

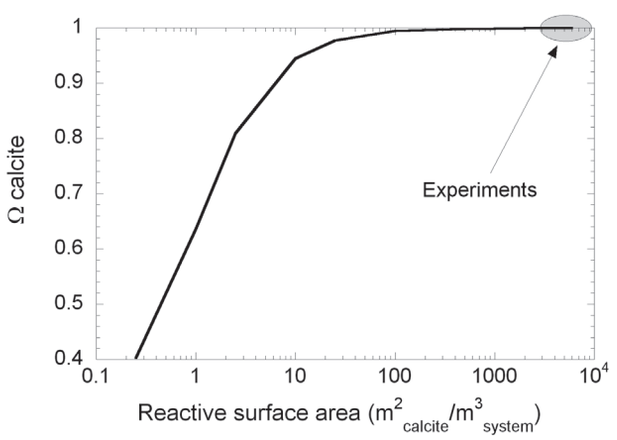

FIGURE 6 | **Variation of calcite saturation state of the outlet solution versus calcite reactive surface area. The values were calculated after simulation of the experimental setting with reactive transport modeling, with a mixing proportion of 15% of saline water (Table 1), and a total flow rate of 0.06mL/min. Note that calcite equilibrium is reached in all the experiments for the reactive surface areas used.**

Figure 7 shows some relevant features of the flow-through experiments. First, dissolution of calcite (calculated from the ΔCa) depends very much on the mixing ratio. Thus, for the same flow rate (Fig. 7B between 0 and 250h), as the mixing ratio increases from 5 to 7.5%, ratio increases from 5 to 7.5%, dissolution of calcite increases from 0.04 to 0.08mmol/kgw, clearly beyond the analytical error (Figure 7D). On the contrary, for the same mixing ratio, dissolution should not depend on the flow rate if equilibrium is reached in a closed system. Thus, a decrease in the flow rate does not affect the Ca concentration significantly beyond the analytical error (Fig. 7 A, C between 150 and 350h). Unlikely, some experiments display a different behaviour. For constant mixing ratio, a drop in the flow rate from 0.09 to 0.045mL/min causes an increase in ΔCa from 0.08 to 0.12mmol/kgw (Fig. 7B and D). This anomalous behaviour suggests that CO_2 diffusion occurs between the reactor cell and the laboratory, as discussed below.

DISCUSSION

The experimental setting allowed an uncontrolled diffusion of CO_2 between the reactor cell and the laboratory atmosphere ($p_{CO2}=10^{-3.22}$ bar). The effect of this diffusion would increase with the residence time in the reactor (i.e. when decreasing the flow rate of the experiment). Although the actual magnitude of CO_2 exchange with the atmosphere in any given experiment is unknown, the functioning of the system falls between two boundary cases: a closed system, where the mixture dissolves calcite with no interaction with laboratory atmospheric CO_2 and a full open system, where the mixture dissolves calcite at laboratory CO_2 pressure. Following earlier discussions, the dissolution of calcite is assumed to reach equilibrium in the two cases. Fig. 8 shows the predicted variation of CO_2 content in the reactor cell with the mixing ratio, after calcite dissolution to equilibrium in

a closed system. On the contrary, for an open system the p_{CO2} will be $10^{-3.22}$bar for any given mixture. For mixing ratios below 17%, the diffusion of CO_2 would take place from the atmosphere to the reaction cell leading to higher pressure of CO_2 a decrease of saturation and higher amount of calcite dissolved. The opposite occurs for mixing ratios above 17%. The grey area in Fig. 8 represents the entire range of possible experimental conditions.

Figure 9 displays the amount of calcite dissolved with the mixing ratio for the two cases discussed. For the closed system, as shown in Fig. 2, dissolution of calcite is maximum for a 50% mixing ratio. For the open system, we can separate two ranges of mixing ratios with a distinctive behaviour. For mixing ratios lower than 17% the gain of CO_2 in the reactor due to diffusion promotes dissolution of calcite. Dissolution increases with CO_2 diffusion, and the process is limited by the CO_2 content in the laboratory atmosphere, i.e., CO_2 pressure in the reactor could never be higher than $10^{-3.22}$ ±10% bar. In contrast, for mixing ratios higher than 17%, diffusion decreases the CO_2 pressure in the reactor cell, causing calcite dissolution to diminish as well. The predicted dissolution of calcite decreases sharply and eventually calcite may precipitate for ratios above 20%. The grey areas in Fig. 9 represent the potential calcite dissolution under the entire possible range of experimental conditions. This limits the areas between the curves of calcite equilibrium for the closed and open systems.

Figure 9 also displays the measured calcite dissolved in each experiment. The highest dissolution corresponds to a mixing ratio of 15% approximately, with an abrupt decrease in fresher and saltier mixtures in the 0-20% mixing range. For higher mixing ratios calcite dissolution is less important. As expected, all the experimental results plot in the grey area of potential calcite dissolution predicted by the calculations. On a closer inspection of the results, the experiments can be grouped according to their residence

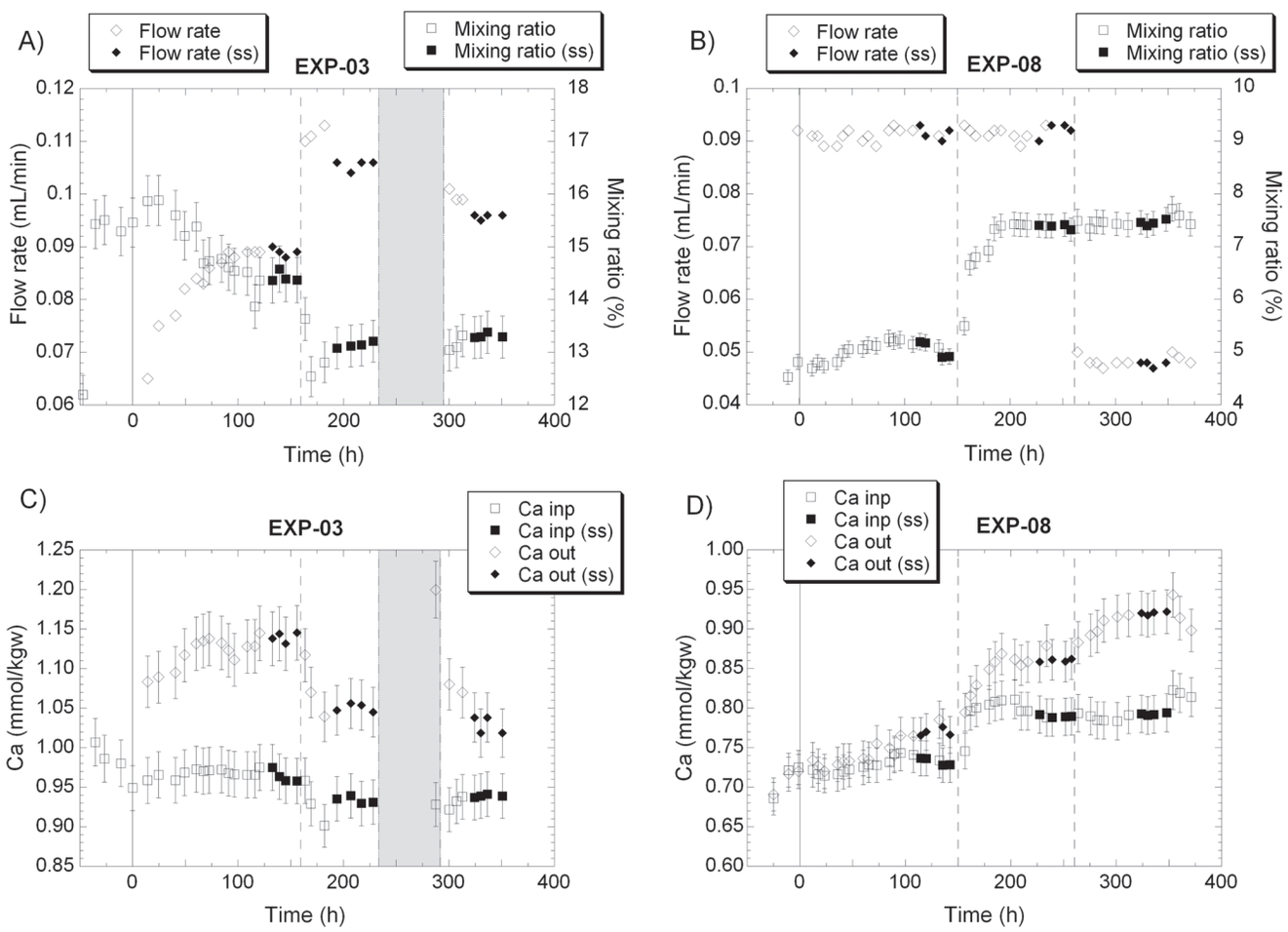

FIGURE 7 | **Variation in flow rate, mixing ratio, and Ca concentration input (computed according to eq. 3) and output (measured), as a function of time in two representative experiments (A and C: EXP-03; B and D: EXP-08). The vertical single line depicts the start of the experiment and the dashed lines represent changes in experimental conditions between the different stages. Grey area indicates conditions of no flow. Data used to calculate average steady state values (ss) are denoted by filled symbols (Table 2).**

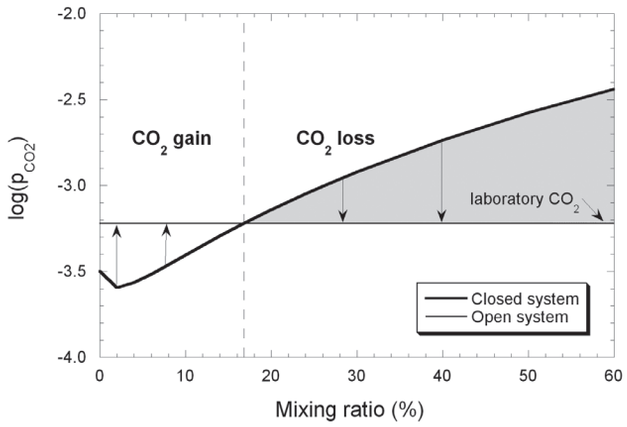

FIGURE 8 | **Predicted variation of CO_2 pressure with the mixing ratio for the systems that are closed and open to the laboratory atmosphere after calcite dissolution to equilibrium. Depending on the mixing ratio, diffusion causes a gain or loss of CO_2 in the reactor cell. Vertical dashed line marks the mixing ratio showing opposite diffusion direction, and the arrows indicate the direction of the CO_2 variation in the reactor cell, from closed to open system. Salinity increases on the right.**

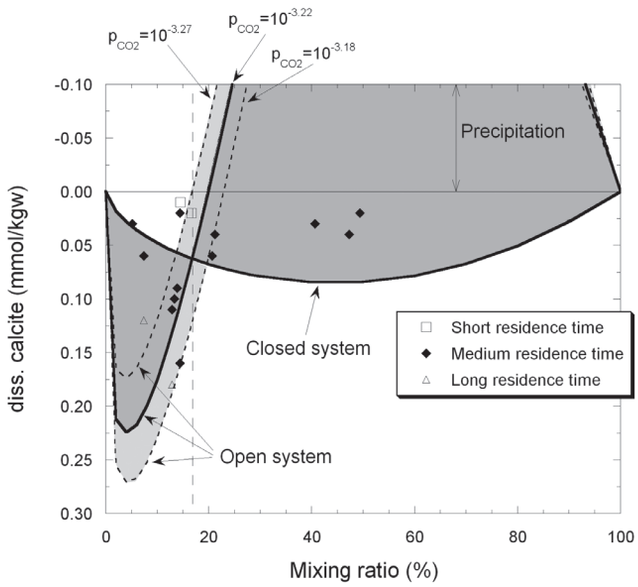

FIGURE 9 | **Comparison of experimental data and simulated values for dissolved calcite. Lines represent the dissolved calcite predicted for dissolution in equilibrium for the open and closed reactor cases. Laboratory atmosphere was $10^{-3.22}$ bar with a 10% error, marked by the curves for $10^{-3.18}$ and $10^{-3.27}$ bar. Grey areas represent the possible ranges for experimental conditions. Vertical dashed line limits the ranges of mixing ratios with gain (below 17%) and loss (above 17%) of CO_2 in the reactor due to CO_2 diffusion.**

time in the reactor. The experiments with longer residence times allow CO_2 to diffuse for a longer time, dissolving more calcite and plotting closer to the predictions for the open system. By contrast, the experiments with short residence times, do not allow much CO_2 diffusion, dissolving less calcite, and plotting close to the predictions for the closed system case.

The high sensitivity of calcite dissolution to small variations of the local p_{CO2} should be noted. For example, as shown by the calculated curves (Fig. 9), a variation of only 10% in the p_{CO2} in solution may result in significant differences in the maximum dissolution at a particular mixing ratio. As a result, it is not easy to determine the real magnitude of calcite dissolution in the field given the difficulties in characterizing the actual p_{CO2} at depth. That is especially challenging in aquifers at poorly characterized areas with degrading organic matter that may alter the geochemistry of groundwater.

CONCLUSIONS

The simulation of mixing waters of different salinities and p_{CO2} in equilibrium with calcite in a system closed to CO_2 exchange with atmosphere shows that saturation is not always a good indicator of the real dissolution potential of the mixture. It is demonstrated that the maximum subsaturation is expected to occur for mixing ratios of about 15%-salty solution, while the expected dissolved calcite reaches its maximum for 50%. This apparent inconsistency is due to the strong influence of the pH in the carbonate speciation, the relative lower activity of CO_3^{2-} compared with that of Ca^{2+}, and to the dependency of the activity coefficients on the mixing ratio (i.e., with the salinity variation). Therefore, the capacity of a given mixture to dissolve calcite should be addressed in terms of calcite dissolution, rather than calcite saturation as commonly done in the literature.

This prediction was tested through a series of flow-through experiments carried out with end-members of different salinity and p_{CO2}, and at different flow rates and for a range of mixing ratios of 0-50%-salty solution. Dissolution of calcite was confirmed by direct observation of the crystal surfaces, and quantified by measuring the release of Ca.

Our experiments displayed a strong dependence of dissolution on the mixing ratio, reaching a maximum for mixing ratios at 15%-salty, and decreasing sharply at higher and lower ratios. These results are consistent with the calcite dissolution predicted by geochemical modeling only if diffusion from/to the laboratory atmosphere CO_2 is taken into account.

Another striking conclusion is the high sensitivity of the amount of calcite dissolved with minor variations of CO_2 pressure at the reaction place. This sensitivity, which was predicted and then confirmed by experiments at different flow rates, could be relevant in field scale interpretations.

Coastal aquifers often contain portions of rich organic matter that may alter the geochemistry of groundwater locally. However, CO_2 pressure measurements in the field are not easy to obtain. Our results imply that this uncertainty may generate very large uncertainties on the prediction of calcite dissolution. Thus, the high sensitivity demonstrated by the geochemical model with respect to the CO_2 content in solution could account for the different and "contradictory" field observations (dissolution vs. lack of dissolution). Therefore, precise measurements of the CO_2 content are of paramount importance in carbonate-mixing water investigation, especially when the modeling results concern geological time scales.

ACKNOWLEDGMENTS

Most of this work has been funded by the European Union (SALTRANS project, contract no. EVK1-CT-2000-00062). E. Sanz is also grateful to a FI doctoral scholarship from the Catalan Government. The authors wish to acknowledge Dr. Jordi Cama for his help and useful comments during the experiments design. All the chemical and SEM analyses were carried out at Serveis Científico Tècnics (Universitat de Barcelona). The authors acknowledge Jordi Delgado and Josep Soler their constructive comments that improved the quality of the paper.

REFERENCES

Arvidson, R.S., Ertan, I.E., Amonette, J.E., Luttge, A., 2003. Variation in calcite dissolution rates: A fundamental problem? Geochimica et Cosmochimica Acta, 67, 1623-1634.

Back, W., Hanshaw, B.B., Herman, J.S., Van Driel, J.N., 1986. Differential dissolution of a Pleistocene reef in the groundwater mixing zone of coastal Yucatan, Mexico. Geology, 14, 137-140.

Back, W., Hanshaw, B.B., Pyle, T.E., Plummer, L.N., Weidie, A.E., 1979. Geochemical significance of groundwater discharge and carbonate solution to the formation of Caleta Xel Ha, Quintana Roo, Mexico. Water Resources Research, 15, 1521-1535.

Corbella, M., Ayora, C., 2003. Role of fluid mixing in deep dissolution of carbonates. Geologica Acta, 1, 305-313.

Corbella, M., Ayora, C., Cardellach, E., 2004. Hydrothermal mixing, carbonate dissolution and sulfide precipitation in Mississippi Valley-type deposits. Mineralium Deposita, 39, 344-357.

Corbella, M., Ayora, C., Cardellach, E., Soler, A. 2006. Reactive transport modeling and hydrothermal karst genesis: The example of the Rocabruna barite deposit (eastern Pyrenees). Chemical Geology, 233, 113-125.

Hanshaw, B.B., Back, W., 1980. Chemical mass-wasting of the northern Yucatan Peninsula by groundwater dissolution. Geology, 8, 222-224.

Harvie, C.E., Moller, N., Weare, J.H., 1984. The prediction of mineral solubilities in natural waters: The Na-K-Mg-Ca-H-Cl-SO_4-OH-HCO_3-CO_3-CO_2-H_2O system to high ionic strength at 25°C. Geochimica et Cosmochimica Acta, 48, 723-751.

Magaritz, M., Luzier, J.E., 1985. Water-rock interactions and seawater-freshwater mixing effects in the coastal dunes aquifer, Coos Bay, Oregon. Geochimica et Cosmochimica Acta, 49, 2515-2525.

Maliva, R.G., Missimer, T.M., Walker, C.W., Owosina, E.S., Dickson, J.A.D., Fallick, A.E., 2001. Carbonate diagenesis in a high transmissivity coastal aquifer, Biscayne Aquifer, Southeastern Florida, USA. Sedimentary Geology, 143, 287-301.

Melim, L.A., Westphal, H., Swart, P.K., Eberli, G.P., Munnecke, A., 2002. Questioning carbonate diagenetic paradigms: Evidence from the Neogene of the Bahamas. Marine Geology, 185, 27-53.

Metz, V., Ganor, J., 2001. Stirring effect on kaolinite dissolution rate. Geochimica et Cosmochimica Acta, 65, 3475-3490.

Ng, K.C., Jones, B., 1995. Hydrogeochemistry of Grand-Cayman, British-West-Indies - Implications for carbonate diagenetic studies. Journal of Hydrology, 164, 193-216.

Parkhurst, D.L., Appelo, C.A.J., 2006. PHREEQC, A hydrogeochemical transport model. Website (2004): http://wwwbrr.cr.usgs.gov/projects/GWC_coupled/phreeqc/

Plummer, L.N., 1975. Mixing of seawater with calcium carbonate groundwater. Geological Society of America Memoir, 142, 219-236.

Plummer, L.N., Vacher, H.L., Mackenzie, F.T., Bricker, O.P., Land, L.S., 1976. Hydrogeochemistry of Bermuda: A case history of ground-water diagenesis of biocalcarenites. Geological Society of America Bulletin, 87, 1301-1316.

Price, R.M., Herman, J.S., 1991. Geochemical investigation of salt-water intrusion into a coastal carbonate aquifer: Mallorca, Spain. Geological Society of America Bulletin, 103, 1270-1279.

Pulido-Leboeuf, P., 2004. Seawater intrusion and associated processes in a small coastal complex aquifer (Castell de Ferro, Spain). Applied Geochemistry, 19, 1517-1527.

Rezaei, M., Sanz, E., Raeisi, E., Ayora, C., Vázquez-Suñe, E., Carrera, J., 2005. Reactive transport modeling of calcite dissolution in the fresh-salt water mixing zone. Journal of Hydrology, 311, 282-298.

Romanov, D., Dreybrodt, W., 2006. Evolution of porosity in the saltwater-freshwater mixing zone of coastal carbonate aquifers: An alternative modelling approach. Journal of Hydrology, 329, 661-673.

Saaltink, M.W., Batlle, F., Ayora, C., Carrera, J., Olivella, S., 2004. RETRASO, a code for modeling reactive transport in saturated and unsaturated porous media. Geologica Acta, 2, 235-251.

Sanford, W.E., Konikow, L.F., 1989. Simulation of calcite dissolution and porosity changes in saltwater mixing zones in coastal aquifers. Water Resources Research, 25, 655-667.

Singurindy, O., Berkowitz, B., Lowell, R.P., 2004. Carbonate dissolution and precipitation in coastal environments: Laboratory analysis and theoretical consideration. Water Resources Research, 40, 1-12.

Smart, P.L., Dawans, J.M., Whitaker, F., 1988. Carbonate dissolution in a modern mixing zone. Nature, 335, 811-813.

Stoessell, R.K., Ward, W.C., Ford, B.H., Schuffert, J.D., 1989. Water chemistry and $CaCO_3$ dissolution in the saline part of an open-flow mixing zone, coastal Yucatan Peninsula, Mexico. Geological Society of America Bulletin, 101(2), 159-169.

Whitaker, F.F., Smart, P.L., 1997. Groundwater circulation and geochemistry of a karstified bankmarginal fracture system, South Andros Island, Bahamas. Journal of Hydrology, 197, 293-315.

Wicks, C.M., Herman, J.S., Randazzo, A.F., Jee, J.L., 1995. Water-rock interactions in a modern coastal mixing zone. Geological Society of America Bulletin, 107, 1023-1032.

Wigley, T.M.L., Plummer, L.N., 1976. Mixing of carbonate waters. Geochimica et Cosmochimica Acta, 40, 989-995.

Manuscript received February 2008;
revision accepted February 2010;
published Online October 2010.